# MODELING IMPACT OF AMPHIPHILIC MACROMOLECULES' DEGREE OF UNSATURATION AND HYDROPHOBE CONFORMATION ON DSPC LIPID BILAYER

By

BIN ZHANG

A thesis submitted to the

Graduate School – New Brunswick

Rutgers, The State University of New Jersey

In partial fulfillment of the requirements

For the degree of

Master of Science

Graduate Program in Chemical and Biochemical Engineering

Written under the direction of

Meenakshi Dutt

And approved by

_____

_____

_____

New Brunswick, New Jersey

October, 2017

**ABSTRACT OF THE THESIS**

Modeling Impact Of Amphiphilic Macromolecules' Degree Of Unsaturation And Hydrophobe Conformation On DSPC Lipid Bilayer

By BIN ZHANG

Thesis Director:

Meenakshi Dutt

As important drug delivery vehicles, liposomes have received extensive attention when being used to encapsulate both hydrophobic and hydrophilic drugs. In order to increase their colloidal stability, poly(ethylene glycol) (PEG) modified amphiphilic molecules(AM) are inserted in the lipid bilayer to form a PEG shell to protect liposomes from aggregation. However, the influence of amphiphile hydrophobic tail unsaturation and hydrophobe conformation are not well studied. Hence in this project, lipid bilayers grafted with a series of AM in different concentrations(2%, 4% and 6%) are built and simulated by using DRY MARTINI Coarse-Grained(CG) Force Field(FF) to capture the impact of amphiphile hydrophobic tail unsaturation and hydrophobe conformation. Our computational research is performed in collaboration with experimental research which synthesized DSPC liposomes with AM to capture the liposome aggregation behavior and membrane permeability. Our finding shows that with the increasing of AM tail unsaturation, there will be more disorders in AM hydrophobic tails. Those disorders decrease the colloidal stability of liposomes. Also with increasing AM concentration in the system, the corona of PEG will be thicker and the distribution of PEG beads becomes more uniform. Those give the

liposome a better protection against each other due to the steric repulsion of PEG. This protection increases the colloidal stability of liposomes and finally make the aggregation of liposomes slower. The outcome of this study combined with experimental results can guide the design of drug delivery liposomes. In addition, the analysis routines developed during the course of this study will contribute to suite of computational tools which is being developed for future studies.

**Acknowledgements**

Pursuing a M.S. degree is a precious experience for me, and I have been fortunate enough to have help and support from many people during the past three years. I would like to thank my thesis advisor, Prof. Meenakshi Dutt for her mentoring, help and trust in my master research life. Since I became a member of the Computational Soft Material Group without any related experience in the area of modeling and simulation, her patient guidance and dedication encourages me to explore, to learn, and to challenge myself. It truly helps a lot in my research path. I truly thank her for all the efforts and suggestions that she made in making me a qualified master student.

I would also like to thank Alysha Moretti and Prof. Kathryn Uhrich for their kind help and suggestions when collaborating with their experiment research. Their insightful ideas, experience and patient explanation of experiment results help me a lot in the adjustments of my computational research.

It's my privilege to have Prof. Charlie Roth and Prof. Kathryn Uhrich as my thesis committee members. I'd like to thank them for accepting my invitation of being my thesis committee. As a graduate coordinator, Prof. Roth's efficient response of both academic and administration questions always help me solve the core issues of these questions. I appreciate his dedication for every single student like me in our department. I want to thank Prof. Uhrich again for overcoming the jet lag in both our previous research meeting and this defense.

I feel grateful for being able to work with so many talented colleagues in our lab, who have made my master studies full of enjoyment and friendship. The help and joy from you guys make our lab a nice family here. I would like to particularly thank Fikret Aydin, Srinivas Mushnoori, Jia Li, Xiaolei Chu for their help and guidance in my master research life.

This thesis is dedicated to my family for financially and spiritually supporting me pursuing a master degree in the US. Without their endless love, I won't reach this stage.

Table of Contents

ABSTRACT OF THE THESIS ..... ii

Acknowledgements ..... iv

Table of Contents ..... vi

List of Tables ..... viii

List of Figures ..... viii

Chapter 1: Introduction ..... 1

Chapter 2: Background ..... 5

Chapter 3: Methodology ..... 7

3.1 Molecular Dynamics ..... 7

3.4 Force Field ..... 10

3.5 System Setup ..... 15

Chapter 4: Results and Discussion ..... 17

4.1 Interfacial Characteristics ..... 17

4.1.1 ROG of PEG ..... 17

4.1.2 Thickness ..... 19

4.1.3 PEG Morphology ..... 21

4.1.4 PEG Bead Density ..... 22

4.2 Hydrophobic Region Characteristics ..... 26

4.2.1 Tail Morphology ..... 26

4.2.2 Chain Order Parameter ..... 27

4.2.3 ROG of Tail ..... 28

Chapter 5: Conclusions ..... 30

Chapter 6: Future Direction ..... 31

Bibliography ..... 32

# List of Tables

Table 3.1 Tabulated Parameters for Nonbonded (Lennard-Jones) Potentials for Different Beads Used in This Study

Table 3.2 Tabulated Parameters for bonded (Harmonic) Potentials for Different Beads Used in This Study

# List of Figures

Figure 3.1 Image of coarse-grained model for DSPC, G18P5_S/O/L, T18P5_S/O/L

Figure 3.2 Image of last frame of grafted DSPC bilayers with different AM concentration and different AM hydrophobic tail unsaturation

Figure 4.1 Simulated average radius of gyration for G18P5_S/O/L(upper) and T18P5_S/O/L(lower) at AM concentration 2%, 4% and 6%

Figure 4.2 Thickness of bilayer corona for G18P5_O/S/L at 2%, 4% and 6%

Figure 4.3 One single G18P5_S in DSPC bilayer at 2 different time point after equilibrium. Only one AM is shown. (a)PEG chain mushroom (b) PEG chain brush

Figure 4.4 snapshot for the upper half of G18P5_S at 2% AM after equilibrium, line A,B,C are three marking lines corresponding to the 3 marking lines in Figure 4.5

Figure 4.5 PEG density vs distance to the mid-plane of DSPC bilayer for G18P5_S at 2%, 4% and 6%, line A,B,C are three marking lines corresponding to the 3 marking lines in Figure 4.4

Figure 4.6 PEG density vs distance to the mid-plane of DSPC bilayer for G18P5_O at 2%, 4% and 6%

Figure 4.7 PEG density vs distance to the mid-plane of DSPC bilayer for G18P5_L at 2%, 4% and 6%

Figure 4.8 AM tail morphology with different unsaturation and backbone

Figure 4.9 AM tail chain order parameter

Figure 4.10 AM tail ROG

# Chapter 1: Introduction

Liposomes are spherical and enclosed phospholipid bilayers. They are important drug delivery mediums that can reduce drug toxicity and improve biocompatibility.[1,2] Liposomes are effective drug carriers due to their ability to store hydrophobic therapeutic molecules in the hydrocarbon region of their bilayer, or hydrophilic drug molecules in the phospholipid polar head group-solvent interface. By loading hydrophobic drug molecules into the lipid hydrocarbon region or bounding hydrophilic drug molecules to the lipid polar head group, these molecules can be effectively delivered in the human body.[3] In order to increase the colloidal stability, poly(ethylene glycol) (PEG) are often used as coating molecules.[4] PEG chains are proved to effectively control the size,[5-7] morphology,[7-9] compressibility,[6,10] encapsulation efficiency[5,11,12] and permeability of liposomes.[5,11] The PEG layer forms a hydrophilic shell that further protects the liposomes from aggregation.[13,14]

Phosphatidylcholine which is usually found in the exoplasmic or outer leaflet of a cell membrane is a major component of cell membranes.[20] It can be used for membrane-mediated cell signaling.[21] This study focus on understanding the influence of Amphiphilic Molecules (AM) with different degrees of unsaturation(stearate, oleate, linoleate) on the colloidal stability and permeability of DSPC liposomes grafted with AM. A collaborative experiment study has been performed for this purpose. 1,2-Distearoyl-sn-glycero-3-phosphocholine(DSPC) is used to synthesize the lipid liposomes here.

The lipid bilayer exists in gel phase with ordered form at low temperature. In gel phase, the phospholipids pack themselves in a hexagonal two-dimensional lattice with the acyl chains in a fully extended conformation. When the temperature increases to high level, the lipid hydrocarbon chains melt and the bilayer forms a liquid-crystal line phase, referred to as the liquid phase.[22-24] The transition temperature of pure DSPC is 328K. However, in both experiment and simulation, our setup our temperature to 310K. The DSPC bilayer or liposome are supposed to be in gel phase at 310K. With the adding of AM, the phase behavior may change at 310K. It is also known that there will be a decrease in the permeability of phospholipid bilayers to solutes when acyl-chain saturation increases.[15-19] Experiment results from W. Rawicz etc. shows that: An unsaturated double bond will induce a kink in the alkane chain, disrupting the regular periodic structure. Extra free space within the bilayer will be created by this disruption, then it makes additional flexibility in the adjacent chains. The disruption of packing leads to lower transition temperatures with increasing double bonds.[22]

The experiment results show that the linoleic AM with induce the aggregation of liposomes at 310K compared to stearic and oleic AM. The hydrophilic drug release rate also increases with unsaturation in AM hydrophobic tails. However, it's hard to directly see what is happening to unsaturated hydrophobic tails and its local environment from experimental results. From computational perspective, the conformations and dynamics of molecules can be resolved by using Molecular Dynamics (MD) simulations. In this study, we design lipid bilayers composed of DSPC lipid and AM with different degrees of unsaturation. We

focus on the local scale of liposome by doing the study on a small bilayer. Our results combined with experimental results can be used to design liposome drug carriers.

From computational perspective, molecular modeling is commonly used to study the properties of PEG and phospholipids in solution. Atomistic force fields are giving high-resolution perspective to researchers, but completely unfeasible for large-scale applications due to computational cost required. For research regarding PEG, this method are constraining PEG with molecular weight smaller than 500 g/mol in a small size simulation box to make computational expense affordable. For long PEG which has molecular weight larger than 500 g/mol needs to be simulated in a large simulation box. The increasing amount of atoms, solvents and all the interactions in the box make the simulation computational expense to reach a large time and length scale. Our system is in gel phase which has a relatively slow dynamics compared to liquid phase. In order to observe the dynamic properties, we need to run the system in a larger time scale.

In order to overcome disadvantage of time and length scale, researchers are also using coarse-grained force fields with explicit solvent to simulate long PEG chains. PEGylated lipids with long chains grafted on membranes or liposomes mean a large simulation box in explicit solvent method in order to avoid cross boundary interaction between PEG chains. A large box means more explicit water there which makes simulation expensive. Besides coarse-grained with explicit solvent, another good solution for computational efficiency is

coarse-grained with implicit solvent which would decrease the number of particle interaction calculations and thus decrease computational cost.

# Chapter 2: Background

MARTINI Coarse-Grained Force Field developed by Marrink et al. is one of the most well used coarse-grain methods that researchers use for biological and chemistry computational studies.[25,26] Its advantages over other coarse-grained models are the possibility to explore faster long time scales and the wider range of applicability. The short-range nature of the interactions speeds up the calculations between 3 times (compared to simulations using typical cutoffs of 1.4 nm, ours are 0.9 nm to 1.2 nm).[25] Thus MARTINI Coarse-Grained model offers a reasonable combination of speed and accuracy. In this study the AM has a PEG chain with molecular weight 5000 g/mol, thus we removed explicit solvent molecules and replacing their influence by implicit solvent potentials for nonsolvent bead to greatly decrease computational cost.[27]

Hwankyu Lee et al. parameterized the MARTINI Coarse-Grained Force Field for PEG developed from CHARMM all-atom FF. They successfully make excellent agreement with neutron scattering results for long coarse-grained PEG (442<Mw<6998) at low concentration in water.[28] Based on the coarse-grained scheme of PEG from Hwankyu Lee et al., Roland Faller studied the influence of pressure environment on the conformations of mixtures of PEGylated and non-PEGylated lipids.[29] Based on the coarse-grained scheme of PEG from Hwankyu Lee et al., Ronald G. Larson et al. developed a molecular dynamic force field for PEG with the implicit solvent DRY MARTINI coarse-grained model. Larson's model yields similar distributions of bond length, angles and radius of gyration on PEG chain length as those observed from explicit solvent model.[30]

Computational researchers using Martini Coarse-Grained Force Field with either explicit or implicit solvents mainly focus on the properties of PEG in pure solvents. Now a question for PEG research is to investigate the dynamic behavior of PEGylated lipids grafted on lipid bilayer. In DRY MARTINI Force Field, due to the missing of explicit solvent, the long PEG chain will stick to the surface of lipid bilayer when they are in interaction range. This makes the DRY MARTINI system hard to represent the correct dynamic property of bilayer grafted with PEG. Thus we design a DRY MARTINI system with WCA potential applied between PEG and lipid beads which overcomes this disadvantage.

The innovation of our study is based on the Coarse-Grain Force Field development of Hwankyu Lee and Ronald G. Larson. We develop and use a DRY MARTINI model of AM to study its properties and interactions with DSPC lipid. Our study focuses on the behavior of AM tail and PEG chain in implicit solvent and the morphology of AM hydrophobic tail with different degrees of unsaturation.

# Chapter 3: Methodology

## 3.1 Molecular Dynamics

The dynamics of the simulation system is captured by using classical molecular dynamics(MD) simulations. The forces in the system are derived from integrating Newton's equation of motion as $F_i=m_ia_i=\nabla_iU$, where $F_i$ is the total force vectors, $m_i$ is the mass, $a_i$ is the acceleration vector of particle I, and U is the potential function. The simulation starts with the initial position of each atom. The potential function is determined by bonded and non-bonded interactions between each atom. Then the Velocity Verlet integration will handle updating the trajectories of atoms, which has better stability, time reversibility and preserves the symplectic form on the phase space compared to the Euler method.[31,32] In this research, we are using Large-scale Atomic/Molecular Massively Parallel Simulator (LAMMPS)[33] which has good scalability with huge number of high-performance computing processors.

The non-bonded interaction are represented by pair potential energy. The van der Waals interaction and electrostatic interactions here are shifted Lennard-Jones (LJ) potential and Coulombic potential with an additional switching function S(r) that ramps the energy and force smoothly to zero between an inner and outer cutoff. with the equation:

$$E_{LJ} = 4\varepsilon \left[ (\sigma/r)^{12} - (\sigma/r)^{6} \right], r < r_c$$

$$E_C = Cq_iq_j/\varepsilon r + Sc(r), r < r_c$$

$$S(r) = C, r < r_1$$

$$S(r)=A/3(r-r_1)^3+B/4(r-r_1)^4+C,\ r_1<r<r_c$$

$$A=(-3E'(r_c))+B/4(r-r_1)4+C,\ r_1<r<r_c$$

$$B=(2E'(r_c)-(r_c-r_1)E''(r_c))/(r_c-r_1)^3$$

$$C=-E(r_c)+1/2(r_c-r_1)E'(r_c)-1/12(r_c-r_1)^2E''(r_c))$$

Where $r_1$ is the inner cutoff; $r_c$ is the outer cutoff. The coefficients A, B, and C are computed by LAMMPS to perform the shifting and smoothing. The function S(r) is actually applied once to each term of the LJ formula and once to the Coulombic formula, so there are 2 or 3 sets of A,B,C coefficients depending on which pair style is used. The boundary conditions applied to the smoothing function are as follows: $S'(r_1) = S''(r_1) = 0$, $S(r_c) = -E(r_c)$, $S'(r_c) = -E'(r_c)$, and $S''(r_c) = -E''(r_c)$, where E(r) is the corresponding term in the LJ or Coulombic potential energy function. Single and double primes denote first and second derivatives with respect to r, respectively. The inner cut off is 9 angstroms, outer cut off is 12 angstroms.

Bonded interaction are represented by using bond potential, angle potential and dihedral potential. The bond potential is harmonic potential with equation from Larson[30]:

$$V_{bond}(b) = （1/2）K_b(b - b_0)^2$$

where $b_0$ is the equilibrium bond distance, $K_b$ is the bond force constant.

The angle potential is equation parameterized from Larson[30]:

$$V_{angle}(\theta) = （1/2）K_\theta(\cos(\theta) - \cos(\theta_0))^2$$

where $\theta_0$ is the equilibrium value of the angle, and K is the angle force constant.

The dihedral potential is equation parameterized from Lee[28]:

$$V_{dihedral}(\varphi) = \Sigma K_{\varphi,i}(1 + \cos(n_i\varphi - \varphi_i))$$

Where $n_i$ and $\varphi_i$ are the multiplicities and offsets, respectively, of the 4 individual dihedral terms, $K_\varphi$ is the dihedral constant.

In DRY MARTINI, due to the missing of explicit solvent, the long PEG chain will stick to the surface of lipid bilayer when they are in interaction range. This makes the DRY MARTINI system hard to represent the correct dynamic property of bilayer grafted with PEG. Thus we design a DRY MARTINI system with Weeks-Chandler-Anderson (WCA) potential applied between PEG and lipid beads which overcomes this disadvantage. By using WCA potential, the repulsive force will make PEG able to move out of the interaction range of bilayer, thus eliminating the stick behavior.

The WCA potential is a popular pair potential. This potential is the Lennard-Jones (LJ) potential, shifted upwards by ε and truncated at the LJ potential minimum of $2^{1/6}$ σ. It is a purely repulsive potential.[34] The equation for WCA potential is:

$$\varphi(r) = 4\varepsilon [ (\sigma/r)^{12} - (\sigma/r)^{6}] + \varepsilon, \; r \leq 2^{1/6}\sigma$$

$$\varphi(r) = 0, \; 0 \; r > 2^{1/6}\sigma$$

By applying WCA potential, it prevents the issue of sticking of PEG chain with membrane.

## 3.4 Force Field

We use a DRY MARTINI Coarse-Grain method which adopts a mapping of 4 heavy atoms to one coarse-grained bead. Chemical compounds of molecules are modeled by mapping different bead types that represent different levels of polarity, hydrogen bond capacities and etc. This form of coarse-graining has been used in other simulations involving membranes and PEG. In order to increase the time and length scale, an implicit solvent method was used with appropriate modification to the model.

By applying this method, we can use coarse-grained beads to build an implicit simulation system. The mapping of all coarse-grained beads except coarse-grained PEG beads is based on the package DRY MARTINI v2.1 developed by C. Arnarez et al.[27] The mapping of PEG coarse-grained force field is based on coarse-grained PEG model developed by Larson. Each coarse-grained PEG bead has a mass of 45 amu, while all other type coarse-grained beads in the system have a mass of 72 amu.

Particles are differentiated into four main types: polar (P), nonpolar (N), apolar (C) and charged (Q). Each type is divided into subtypes either using letters to define the hydrogen-bonding capabilities (d for donor, a for acceptor, da for both and 0 for none) or numbers to show the degree of polarity (from I for low polarity to V for high polarity). One single DSPC molecule is coarse-grained into fourteen coarse-grained beads, including one

positively charged head bead (Q0), one negatively charged head bead (Qa), two nonpolar head beads (Na) and ten tail beads (C1). AM molecule PEG part is coarse-grained into 110 PEG bead.[27,30,35] There are two tail conformations in this study, glycerol type AM and tartaric type AM. Both G18P5_S and T18P5_S are coarse-grained into four nonpolar head beads (Na), ten tail beads (C1) and 110 PEG beads (SNda). Both G18P5_O and T18P5_O are coarse-grained into four nonpolar head beads (Na), eight tail beads (C1), two unsaturation tail beads (C3) and 110 PEG beads (SNda). Both G18P5_L and T18P5_L are coarse-grained into four nonpolar head beads (Na), six tail beads (C1), four unsaturation tail beads (C3) and 110 PEG beads (SNda). All molecules are represented by the bead-spring model, as shown in Figure 3.1.

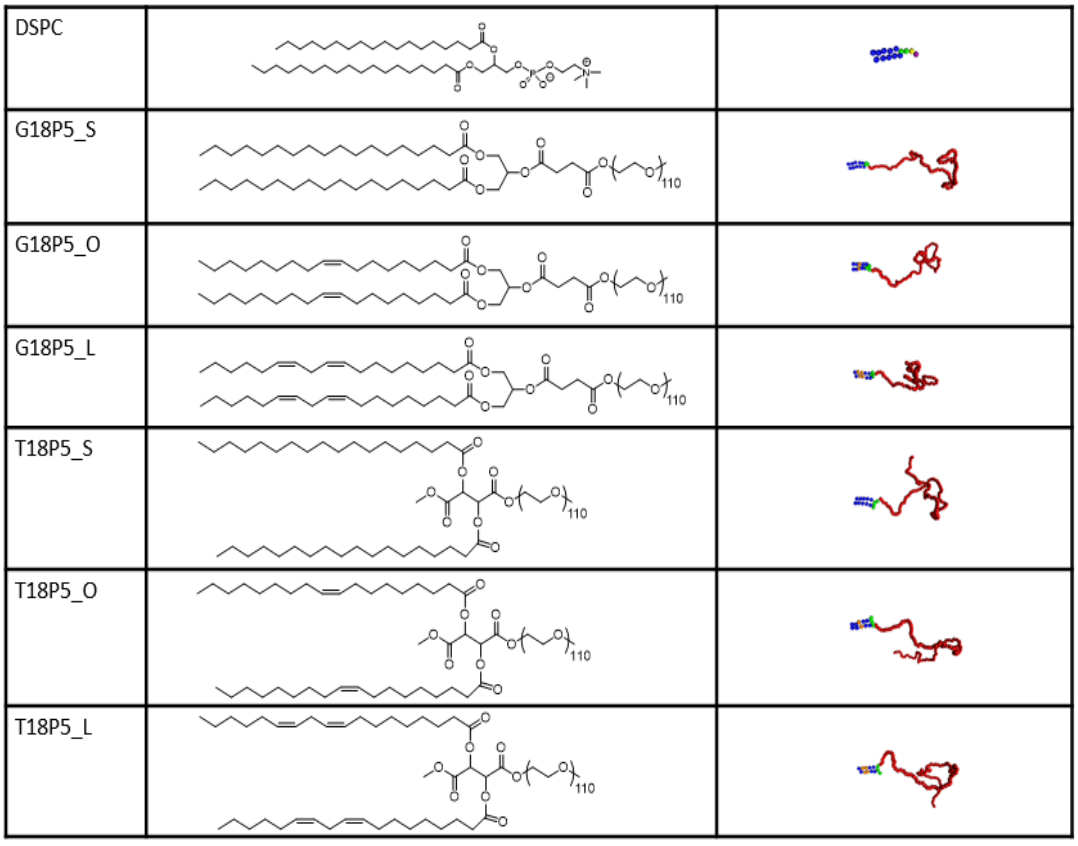


Figure 3.1 Image of coarse-grained model for DSPC, G18P5_S/O/L, T18P5_S/O/L

The DRY MARTINI Force Field with implicit solvent is parameterized by Marrink.[27] Specifically, the non-boned interaction between PEG and any other bead type is captured by using Weeks-Chandler-Andersen potentials to validate the missing of water influence between them in implicit solvent method. The enthalpic penalty of unfavorable interactions between the PEG chain and DSPC avoids the sticking behavior between them due to the missing of explicit solvent. Generally, for the non-bonded interaction between any two bead type is described by using a simple 6-12 Lennard-Jones potential that is shifted to 0 from 0.9 to 1.2 nm. The details for the force field is in Table 3.1.

| | interaction potential | |
|---|---|---|
| LJ | σ (nm) | ε (kJ/mol) |
| Qa-Qa | 0.60 | 2.0 |
| Qa-Na | 0.47 | 0.5 |
| Qa-C1 | 0.62 | 2.0 |
| Qa-C3 | 0.47 | 0.5 |
| Qa-Snda | 0.47 | 0.5 |
| Qa-Qo | 0.60 | 2.0 |
| Na-Na | 0.47 | 2.3 |
| Na-C1 | 0.47 | 2.7 |
| Na-C3 | 0.47 | 2.7 |

| | | |
|---|---|---|
| Na-Snda | 0.47 | 2.7 |
| Na-Qo | 0.47 | 0.5 |
| C1-C1 | 0.47 | 4.5 |
| C1-C3 | 0.47 | 4.5 |
| C1-Snda | 0.47 | 2.7 |
| C1-Qo | 0.62 | 2.0 |
| C3-C3 | 0.47 | 4.5 |
| C3-Snda | 0.47 | 2.7 |
| C3-Qo | 0.47 | 0.5 |
| SNda-SNda | 0.43 | 2.0 |
| SNda-Qo | 0.47 | 0.5 |
| Qo-Qo | 0.60 | 2.0 |

Table 3.1 Tabulated Parameters for Nonbonded (Lennard-Jones) Potentials for Different Beads Used in This Study

| **bond** | k(kJ/mol/nm$^2$) | d(nm) |
|---|---|---|
| np | 1250 | 0.45 |
| Pg1 | 1250 | 0.45 |

| | | |
|---|---|---|
| gg | 1250 | 0.37 |
| cc | 1250 | 0.48 |
| PEG | 16000 | 0.33 |
| **angle** | kθ (kJ/mol/rad2) | θ (deg) |
| pgg | 25.0 | 120 |
| pgc | 25.0 | 180 |
| adc | 45.0 | 180 |
| gcc | 35.0 | 180 |
| ccc | 35.0 | 180 |
| cdc | 45.0 | 120 |
| PEG | 80 | 150 |
| **dihedral** | Kφ (kJ $mol^{-1}$) | φθ (deg) |
| n1 | 1.96 | 180 |
| n2 | 0.18 | 0 |
| n3 | 0.33 | 0 |
| n4 | 0.12 | 0 |

Table 3.2 Tabulated Parameters for bonded (Harmonic) Potentials for Different Beads Used in This Study

The bonded interactions are described by weak harmonic stretching and bending potentials. Also, we used cosine squared potential as angle potentials and charm dihedral potential (in

Table 3.2) to get reasonable radii of gyration for PEG. However, the dihedral potential here limits the time step to no longer than 1 fs in LAMMPS.

## 3.5 System Setup

We begin with a preassembled DSPC bilayer encompassing a specific AM molecule (G/T) present in a fixed concentration (that is, 2%, 4 % or 6%). The total number of molecules constituting the bilayer is 984. The bilayer is placed in a simulation box of dimensions 16 nm x 16 nm x 80 nm with three dimensional periodic boundary conditions. The system is initially run in the canonical ensemble with a temperature of 310 K and a pressure of 1 Bar for 100 ns to get a tensionless bilayer. Then the system is further run for another 100 ns using the canonical ensemble with a constant volume at a temperature of 310 K. After the equilibration phase, the system is run for a further 6 ns to perform various measurements. The phase diagram for all systems at the last frame is shown in Figure 3.2.

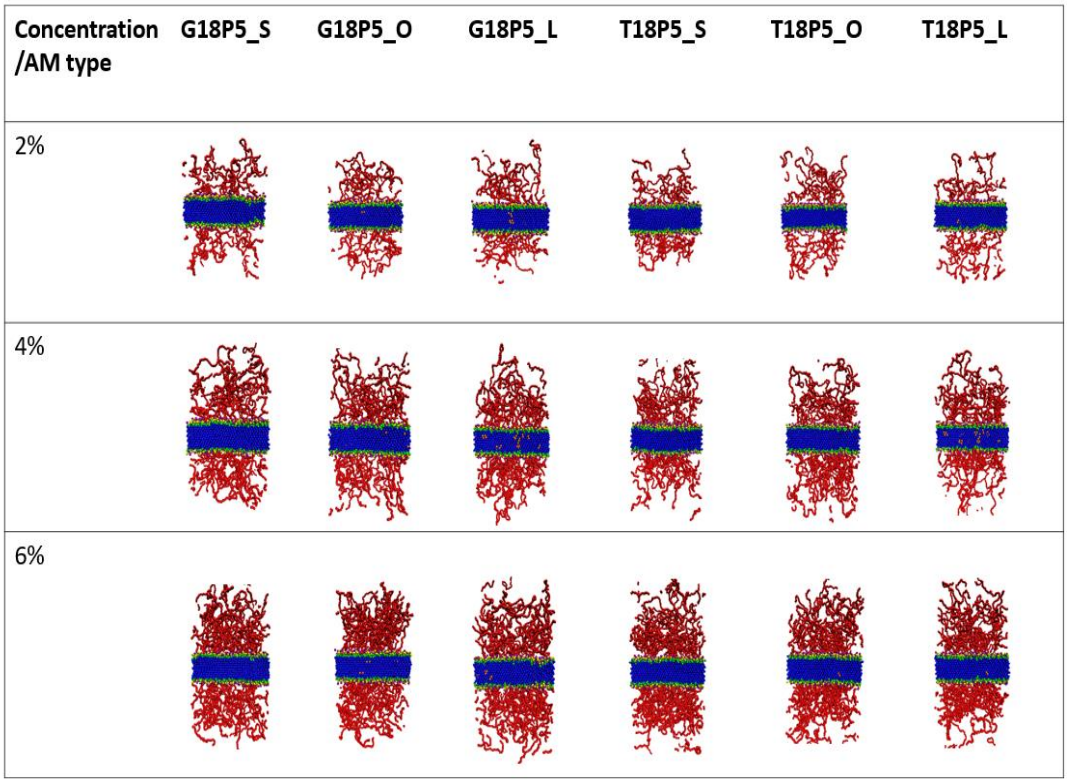


Figure 3.2 Image of last frame of grafted DSPC bilayers with different AM concentration and different AM hydrophobic tail unsaturation

# Chapter 4: Results and Discussion

All the quantitative results are calculated in a self-developed package(MPEG) coding in VC++.

## 4.1 Interfacial Characteristics

### 4.1.1 ROG of PEG

Radius of gyration (ROG) is a measurement of the size of the group of atoms that accommodates simulation model with real world PEG morphology. It's defined as:

$$R_g^2=(1/N)\ \Sigma(r_i-r_{cm})^2$$

where N is the total number of PEG beads in one single AM, $r_{cm}$ is the center-of-mass position of the group, and the sum is over all atoms in the group. The final results are averaged over all AM in each system. The ideal PEG chain regime from experiment results is following the equation:

$$R_g= 0.02M_w^v,$$

where $M_w$ is the molecular weight of PEG chain, v= 0.610 for the Larson implicit model, v=0.583 for experimental value.[28,36] Thus the Larson implicit ROG should be 35 angstroms, experimental ROG should be 28 angstroms.

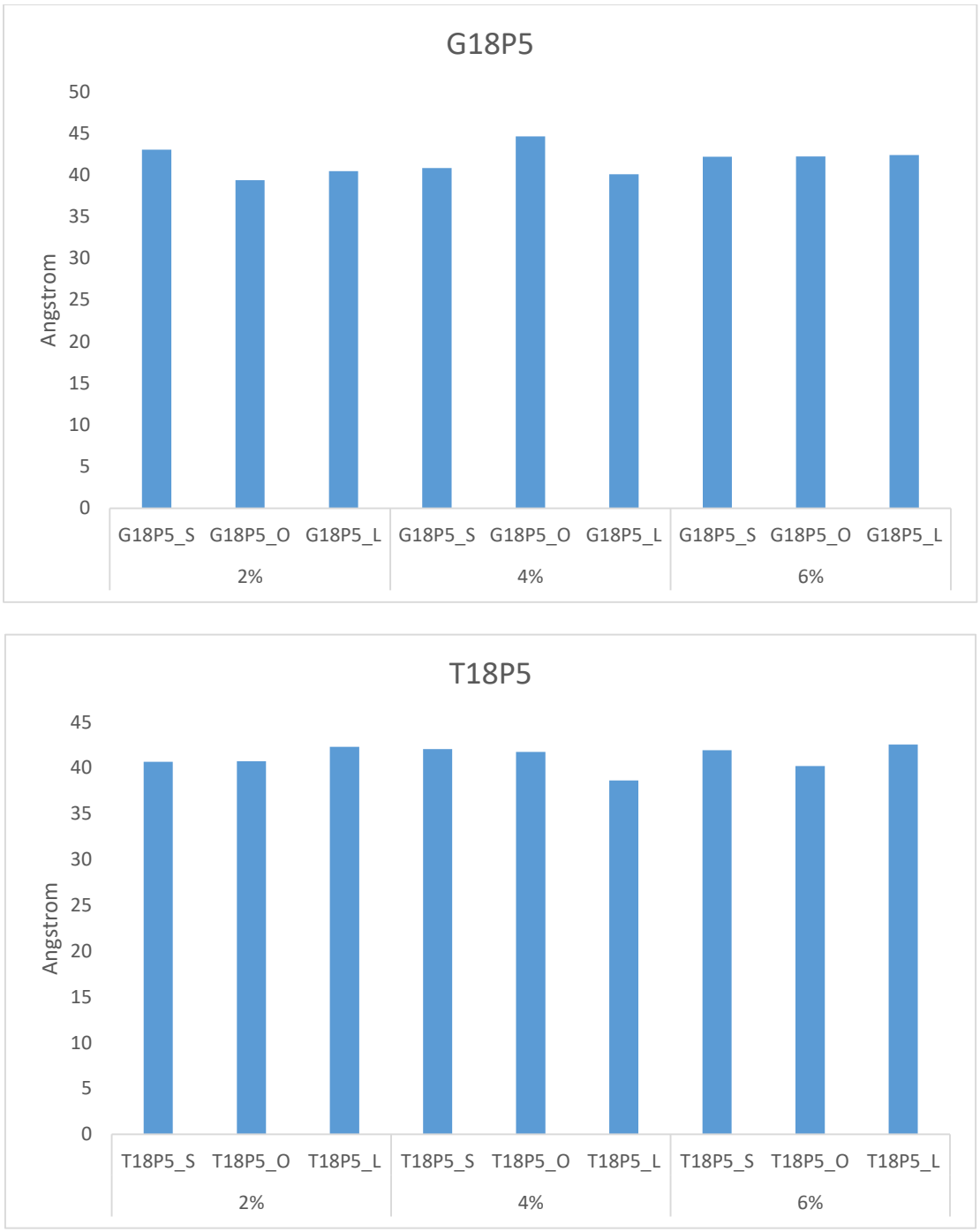


Figure 4.1 Simulated average radius of gyration for G18P5_S/O/L(upper) and T18P5_S/O/L(lower) at AM concentration 2%, 4% and 6%

The results show that after validating of our model, the simulated ROG for PEG110 in bilayer has an acceptable agreement with the ideal ROG value. The results also show that

the ROG is not affected by the concentration, tail unsaturation and tail conformation of AM.

### 4.1.2 Thickness

The PEG chains in the AM molecules adopt orientations that minimize the free energy of the system by maximizing their conformational and configurational entropy. The thickness of each single PEG chain can be calculated by determining the distance between maximum and minimum z coordinates of each single PEG chain. The thickness of the PEG corona is measured by averaging over the thickness of all the peg chains constituting the corona. Then the thickness of PEG corona is calculated by averaging the thickness of all PEG chains in one monolayer. The equation is: H=mean(Zmax-Zmin), where H is the corona thickness, Zmax and Zmin are the maximum and minimum z coordinated of a single PEG chain. This measurement is performed for bilayers encompassing different types and concentrations of the AM molecules (see Figure 4.2).

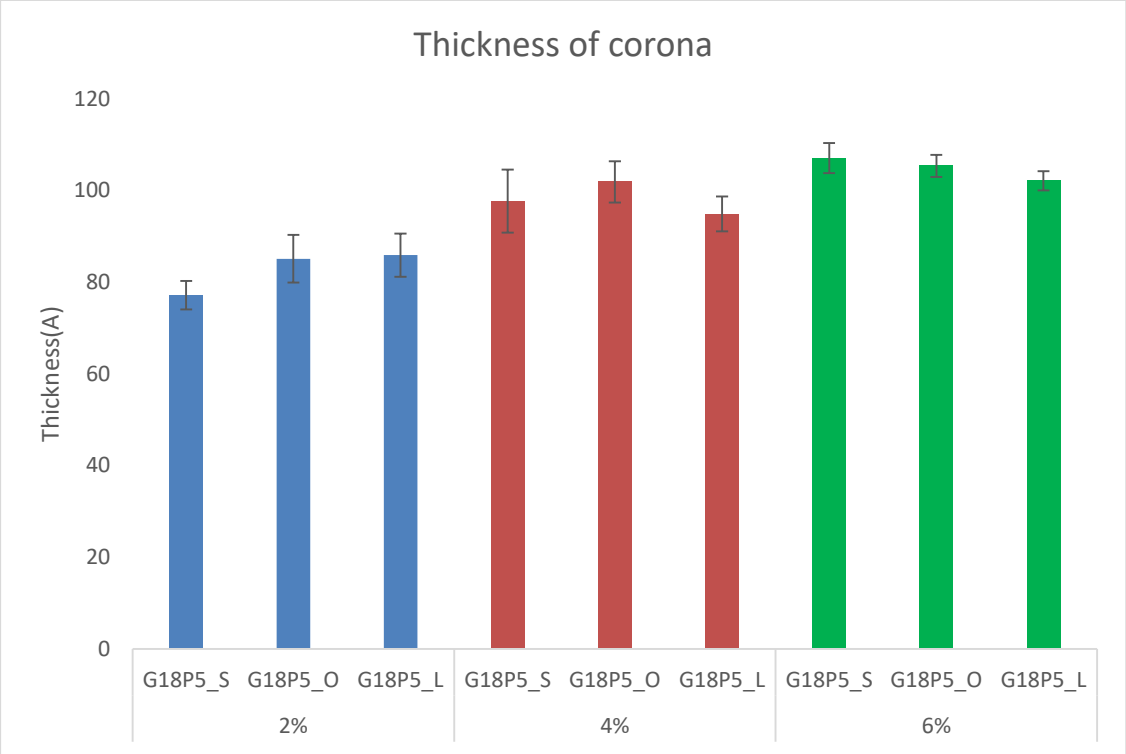


Figure 4.2 Thickness of bilayer corona for G18P5_O/S/L at 2%, 4% and 6%

Our results show the thickness of the PEG corona to increase with increasing concentration of the AM molecules. The higher concentrations of the AM molecules induce the PEG chains to adopt brush-like conformations. This enables the individual PEG chains to maximize their conformational entropy under constraints of reducing area per AM molecule. As a consequence, the PEG corona is thicker with increasing concentration of AM molecules. Based on this observation, we can predict that in experiments, liposomes with the higher concentration of AM molecules also have a thicker PEG corona. The PEG chains are known to prevent the liposomes from aggregating with each other. Hence, an increasing thickness of the PEG layer increase the barrier to aggregation, thereby improving the stability of the PEG-grafted liposome. These results are in good agreement with experimental observations which demonstrate liposomes with lower concentration of

AM molecules to have a higher tendency to aggregate. Hence, the PEG corona serves to increase the colloidal stability of the liposomes.

### 4.1.3 PEG Morphology

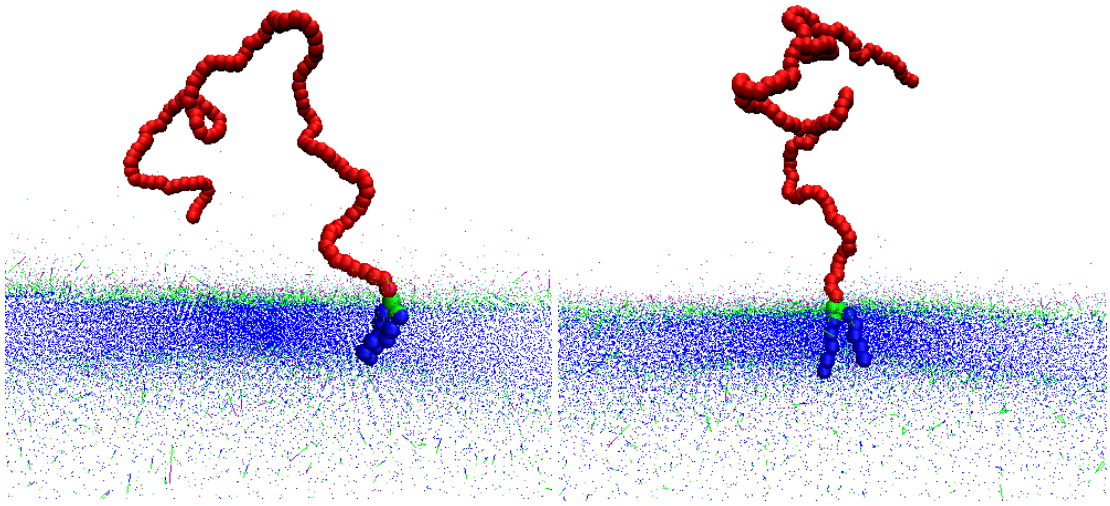

Figure 4.3 One single G18P5_S in DSPC bilayer at 2 different time point after equilibrium. Only one AM is shown. (a)PEG chain mushroom (b) PEG chain brush

The morphology of the PEG chains also provide insight into their role in enhancing the stability of the liposomes. Figure 4.3 shows mushroom and brush conformations of the PEG chains. The mushroom conformation is adopted primarily by the PEG chains for low concentration of the AM molecules. Where as the brush conformations are adopted for higher concentration of the AM molecules. Analogous to an earlier study [28], each PEG chain strives to maximize its conformational entropy. However, the spacing between two neighboring AM molecules impacts the conformation of the PEG chains. For closely spaced or high concentration of AM molecules, the PEG chains adopt a brush-like conformation. Brush-like conformations of the PEG chains shield the bilayer surface from neighboring liposomes and prevent their aggregation. For AM molecules with larger space

between themselves (or low concentration of AM molecules), the PEG chains adopt mushroom-like conformations. The mushroom-like conformation of the PEG chains are much more likely to expose the bilayer surface to approaching liposomes, thereby enabling their aggregation.

### 4.1.4 PEG Bead Density

Here we introduce the PEG bead density measurement. The upper half of simulation box is divided into 160 equal size slabs in the z axis. The thickness for each slab is 5 Angstroms. Then we calculate probability of PEG beads in each slab over a time interval of 6ns. The results are normalized by total number of beads in the whole upper half simulation box.

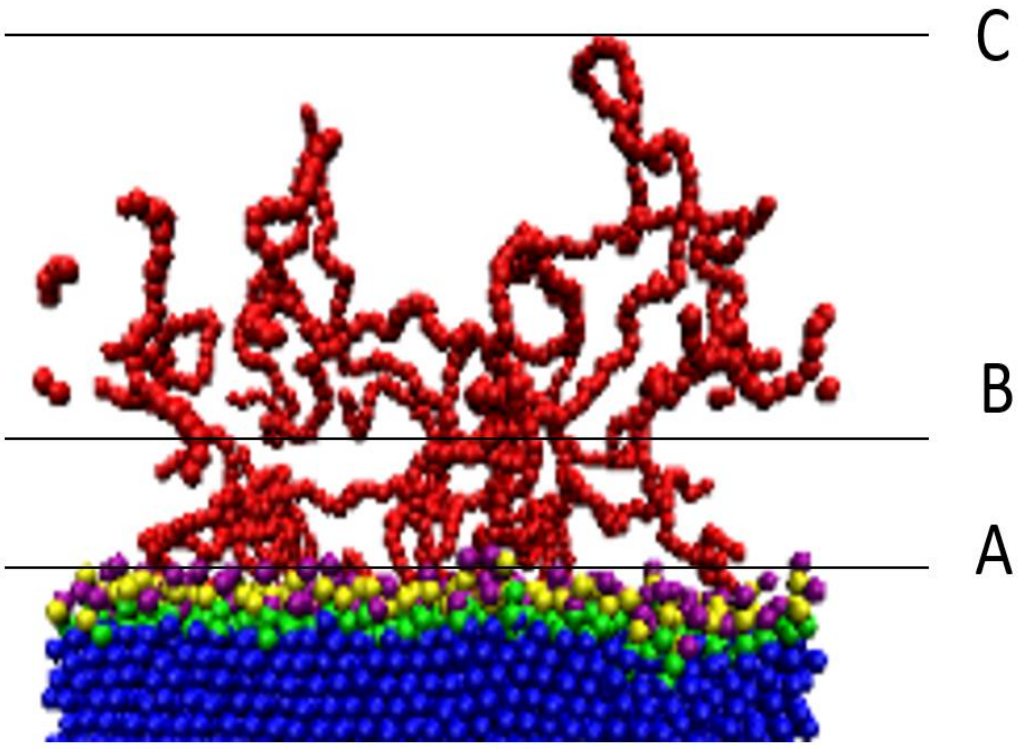


Figure 4.4 snapshot for the upper half of G18P5_S at 2% AM after equilibrium, line A,B,C are three marking lines corresponding to the 3 marking lines in Figure 4.5

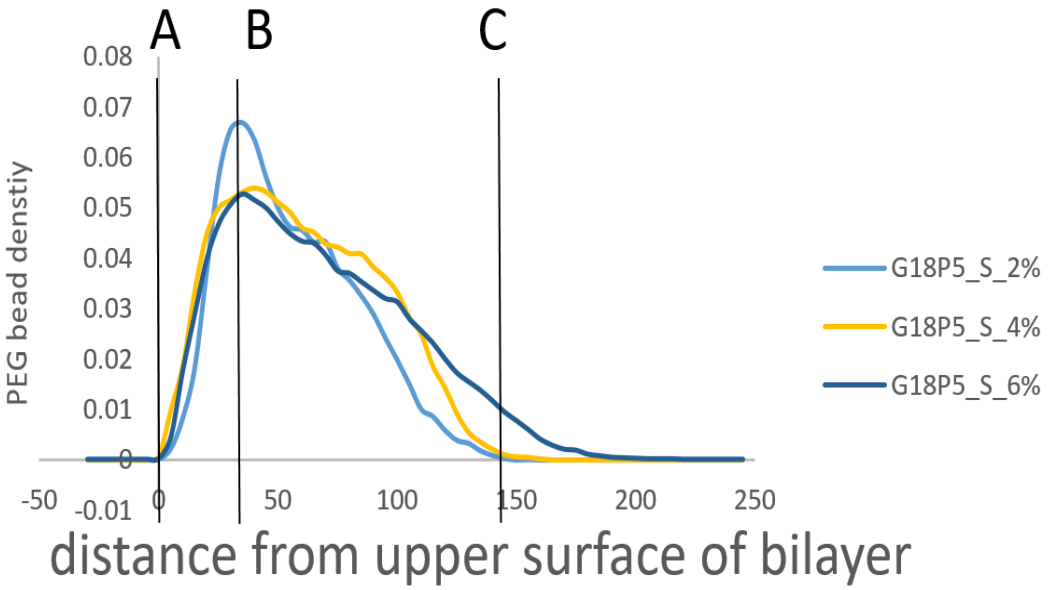


Figure 4.5 PEG density vs distance to the mid-plane of DSPC bilayer for G18P5_S at 2%, 4% and 6%, line A,B,C are three marking lines corresponding to the 3 marking lines in Figure 4.4

Figure 4.4 and Figure 4.5 show that for G18P5_S, 2% AM is denser at the lower layers of corona than 4% and 6% and less denser at higher layers of corona than 4% and 6%. The shape of 4% and 6% are smoother than 2%, which means that the distribution of PEG beads in corona of PEG layer is more uniform.

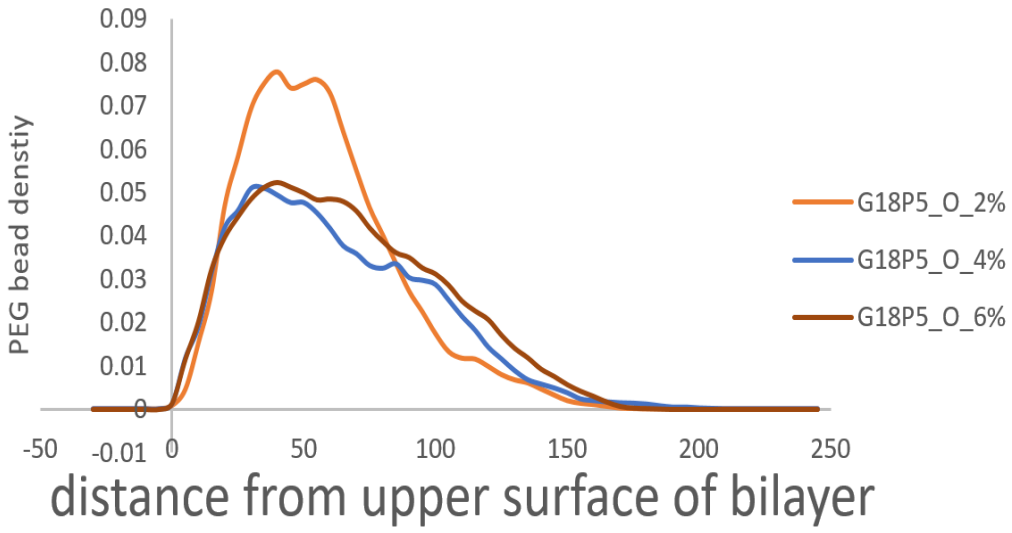


Figure 4.6 PEG density vs distance to the mid-plane of DSPC bilayer for G18P5_O at 2%, 4% and 6%

Figure 4.6 shows that for G18P5_O, we see similar results or trend like G18P5_S.

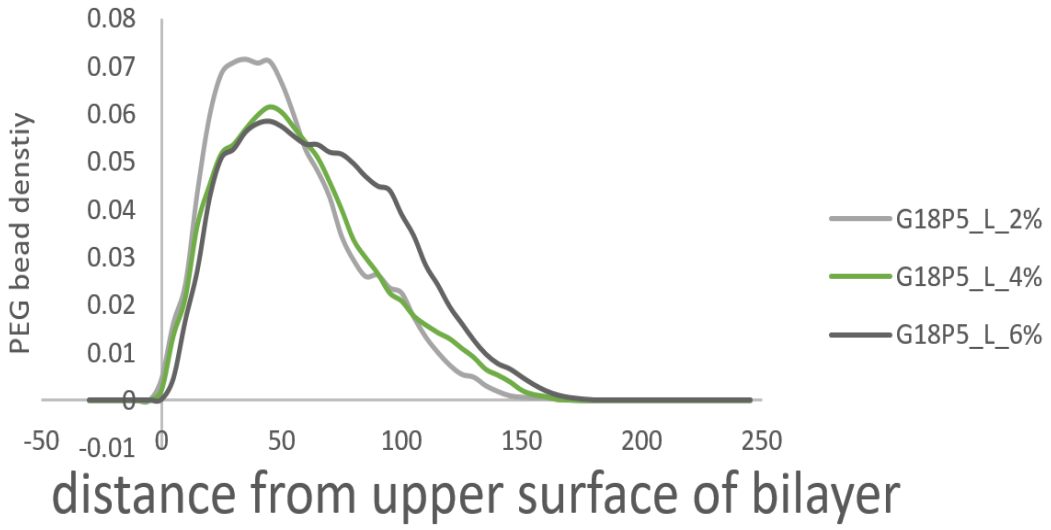


Figure 4.7 PEG density vs distance to the mid-plane of DSPC bilayer for G18P5_L at 2%, 4% and 6%

Figure 4.7 shows that for G18P5_L, we see similar results or trend like G18P5_S and G18P5_O. 2% AM is denser at the lower layers of corona than 4% and 6% and less denser at higher layers of corona than 4% and 6%. The higher AM grafting density, the lateral volume available to each PEG chain will be smaller (brush shape). Mushroom shape will make the lower layer of corona dense, brush shape will make higher layer of corona dense. For higher grafting densities of PEG, due to more stretched out conformations (brush shape) of the PEG chain, the bead densities at the higher layers will be greater than those corresponding to lower grafting densities. In addition, the PEG beads density remains nonzero for higher levels of the corona for 6% concentration of the AM molecules (in comparison to the 4%). A more uniformly distributed PEG corona at high AM concentration endows liposomes greater stability from aggregation. These findings are in good agreement with our experimental observations.

## 4.2 Hydrophobic Region Characteristics

### 4.2.1 Tail Morphology

Experimental results show the permeability of the liposomes to be increasing for AM molecules with higher number of double bonds and present in larger concentrations. We hypothesize that this is caused local disorder induced in the bilayer by the AM molecules. Figure 4.8 shows the chain conformations for AM molecules with different backbone structure and degrees of unsaturation. For AM molecules with no double bonds in the hydrocarbon tails, the tails have very little disorder and are well packed in the DSPC bilayer which is the gel phase. This is expected as the backbone chemical structure for G18P5_S tail is identical to the hydrocarbon tails of DSPC. The disorder in the hydrocarbon tails become stronger with the number of double bonds. In addition, the excluded volume of the hydrocarbon tails increases with the number of double bonds. The excluded volume of the hydrophobic component of the AM molecule will affect the packing and the tail conformations of the neighboring lipids. Hence, the disorder in the hydrocarbon tails of the AM molecules disrupts the tails of the lipids in their vicinity, thereby inducing a local fluid phase. This effect is surmised to become stronger with increasing number of double bonds in the hydrocarbon tails of the AM molecules. As a consequence, the bilayer stability decreases with increasing number of double bonds in the hydrocarbon tails and concentration of the AM molecules. Hence, for G18P5_O and G18P5_L, the disorder of the AM hydrocarbon tails impacts the stability of the bilayer.

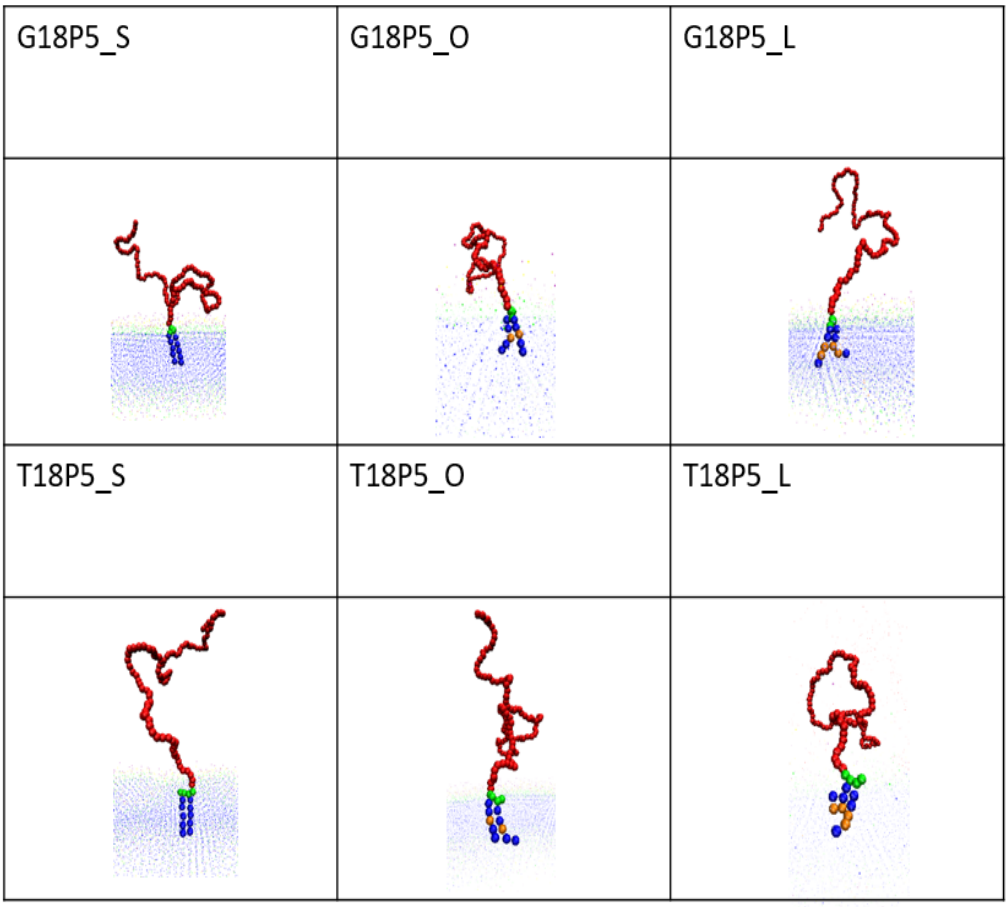


Figure 4.8 AM tail morphology with different unsaturation and backbone

### 4.2.2 Chain Order Parameter

The chain order parameter is defined as s = (3(cos2 θ) - 1)/2, where θ is the angle between the membrane normal and the vector joining the first and the last hydrophobic tail bead on one single tail.[37] According to the equation, a large chain order parameter represents a small tilt angle θ of the lipid. The measurement of chain order parameter can be used to capture the fluidity properties of the membrane. From previous observation, we can see that with

the increasing numbers of carbon double bonds, the disorder of AM tails are increasing. Thus the vicinity lipid around AM should be disturbed more and have a larger tilt angle.

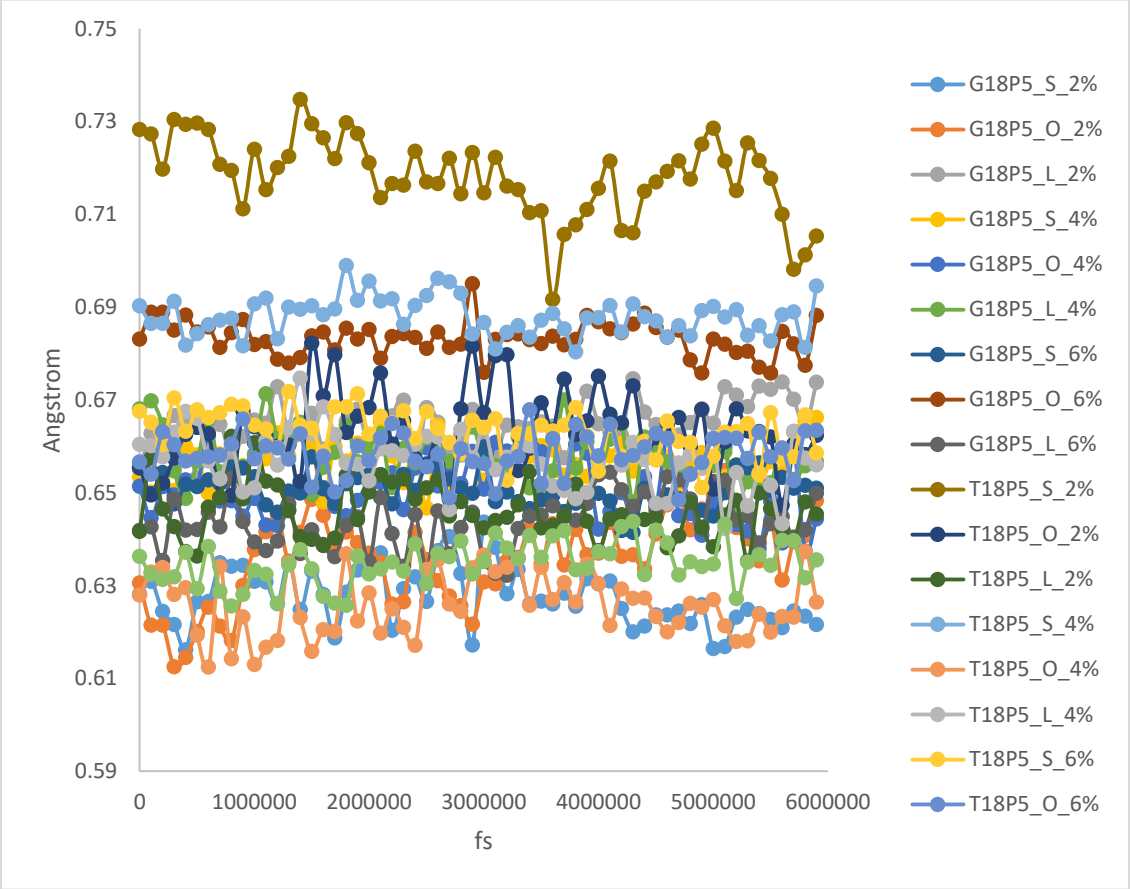


Figure 4.9 AM tail chain order parameter

However, based on the measurement results in figure 4.9, there is no reasonable trend or pattern observed here. Anyway this function in MPEG can be used in future research.

### 4.2.3 ROG of Tail

Same logic and method as the measurement of PEG ROG, but the tail ROG is calculated over all the hydrophobic tail beads in each single AM in the package MPEG. Due to the

increasing disorder with the increasing of carbon double bonds, the AM tail wants more space around it to maximize the conformation entropy. The expected results are that the tail ROG will increase with the increasing tail disorder. However, shown in figure 4.10 there is no reasonable trend or pattern observed here. This function of MPEG can be used in the future for other systems.

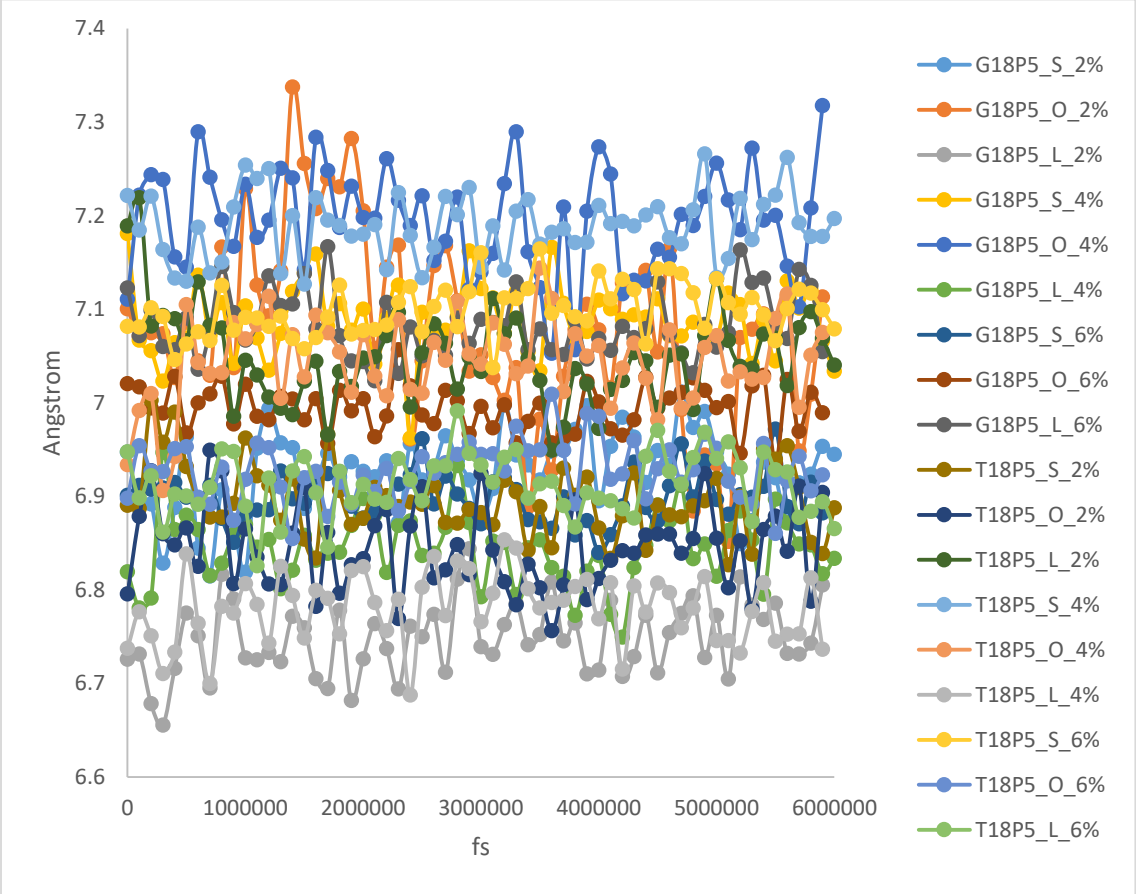


Figure 4.10 AM tail ROG

# Chapter 5: Conclusions

By utilizing DRY MARTINI Coarse-Grained Force Field, we performed simulations on Modeling Impact of amphiphilic macromolecules' degree of unsaturation and hydrophobe conformation on DSPC lipid bilayer. All systems are simulated in canonical NPT ensemble for 100ns at 310K and in NVT for 100ns at 310K. The movies and measurements are done over 6ns after equilibrium. Our results indicate that with the increasing concentration of AM in bilayer, the corona of PEG will become thicker and more uniformly distributed, thus make the aggregation between liposomes harder due to the increasing of colloidal stability. One of the factors contributing to this observation is the transition from mushroom to brush-like conformations of the PEG chains with increasing concentration of the AM molecules. Increasing concentrations of AM molecules with higher number of double bonds induce greater local disorder in the neighboring lipids. The local disorder decreases the stability of the bilayer and increases the permeability of the liposomes, thereby reducing their colloidal stability. The analysis routines (compute package MPEG) developed during the course of this study will contribute to suite of computational tools which is being developed for future studies.

# Chapter 6: Future Direction

Future simulations are designed for the free energy perturbation regarding the influence of tail unsaturation and conformation. By comparing the potential of mean force(PMF) when pulling one single AM out of the bilayer along the pulling coordinates, we will be able to observe the influence of unsaturation and conformation on the stability of bilayer. A relative small energy it takes to pull one single AM out of the membrane means that the AM doesn't like to stay in the membrane. The membrane with this kind of AM has a lower stability compared to those who take relatively large energy to pull. The AM with high unsaturation and tartaric type is supposed to have a low stability and takes smaller energy to pull.

The sampling will be done in Umbrella Sampling(US). At the beginning, the pulling will be carried out to create a set of starting configurations, one for each 'window' to be used in the weighted histogram free energy calculations. The pulling rate used in this stage is sufficiently slow to allow the average position of the surfactant to keep up with the position of the minimum in the pulling potential. Then run sufficient long simulations in each window with a harmonic force applied for each window. Then use the weighed histogram analysis method (WHAM) to generate the PMFs. Master student Akash Banerjee will work on the current model accomplishment.

# Bibliography

[1] Samad, A.; Sultana, Y.; Aqil, M. Liposomal drug delivery systems: an update review, Curr. Drug Deliv. 4 (2007) 297–305.

[2] Allen, T.M.; Cullis, P.R. Liposomal drug delivery systems: from concept to clinical applications, Adv. Drug Deliv. Rev. 65 (2013) 36–48.

[3] Khan, D.R.; Rezler, E.M.; Lauer-Fields, J.; Fields, G.B. Effects of drug hydrophobicity on liposomal stability, Chem. Biol. Drug Des. 71 (2008) 3–7.

[4] Immordino, M.L.; Dosio, F.; Cattel, L. Stealth liposomes: review of the basic science, rationale, and clinical applications, existing and potential, Int. J. Nanomed. 1 (2006) 297–315.

[5] Nicholas, A.R.; Scott, M.J.; Kennedy, N.I.; Jones, M.N. Biochim. Biophys. Acta 1463 (2000) 167–178.

[6] Garbuzenko, O.; Barenholz, Y.; Priev, A. Chem. Phys. Lipids 135 (2005) 117–129.

[7] Lee, H.; Pastor, R.W. J. Phys. Chem. B 115 (2011) 7830–7837.

[8] Bru, M.R.; Thompson, D.H.; Szleifer, I. Biophys. J. 83 (2002) 2419–2439.

[9] Sandstrom, M. C.; Johansson, E.; Edwards, K. Langmuir 23 (2007) 4192–4198.

[10] Stepniewski, M.; Gierula, M.P.; Rog, T.; Danne, R.; Orlowski, A.; Karttunen, M.; Urtti, A.; Yliperttula, M.; Vuorimaa, E.; Bunker, A. Langmuir 27 (2011) 7788–7798.

[11] Kasbauer, M.; Lasic, D. D.; Winterhalter, M. Chem. Phys. Lipids 86 (1997) 153–159.

[12] Lee, H.; Kim, H. R.; Park, J. C. Phys. Chem. Chem. Phys. 16 (2014) 3763.

[13] Harrington, K. J.; Rowlinson-Busza, G.; Syrigos, K. N.; Uster, P. S.; Vile, R. G.; Stewart, J. S. W. Pegylated liposomes have potential as vehicles for intratumoral and subcutaneous drug delivery, Clin. Cancer Res. 6 (2000) 2528–2537.

[14] Hui, S. W.; Kuhl, T. L.; Guo, Y. Q.; Israelachvili, J. Use of poly(ethylene glycol) to control cell aggregation and fusion. Colloids and Surfaces B: Biointerfaces 14 (1999) 213-222.

[15] Gier, J. de; Mandersloot, J. G.; van Deenen, L. L. M. Lipid composition and permeability of liposomes, Biochim. Biophys. Acta, 150 (1968) 666-675.

[16] Scarpa, A.; Gier, J. de. Cation permeability of liposomes as a function of the chemical composition of the lipid bilayer, Biochim. Biophys. Acta, 241 (1971) 789- 797.

[17] Blok, M.C.; vander Neut-Kok, E. C. M.; van Deenen, L. L. M.; Gier, J. de. The effect of chain length and lipid phase transitions, Biochim. Biophys. Acta, 406 (1975) 187-196.

[18] Subczynski, W. K.; Wisniewska, A.; Yin, J. J.; Hyde, J. S.; Kusumi, A. Hydrophobic Barriers of Lipid Bilayer Membranes Formed by Reduction of Water Penetration by Alkyl Chain Unsaturation and Cholesterol. Biochemistry 1994, 33, 7670-7681.

[19] Thakkar, M. F.; Ayappa, K. G. Effect of polymer grafting on the bilayer gel to liquid-crystalline transition. J. Phys. Chem. B 2010, 114, 2738−2748.

[20] Wirtz, K. W. Phospholipid transfer proteins. Annu. Rev. Biochem. 1991, 60 (13): 73–99.

[21] Kanno, K.; Wu, M. K.; Agate, D. A.; Fanelli, B. K.; Wagle, N.; Scapa, E. F.; Ukomadu, C.; Cohen, D. E.; Interacting proteins dictate function of the minimal START domain phosphatidylcholine transfer protein/StarD2 (2007). J. Biol. Chem. 282 (42): 30728–36.

[22] Rawicz, W.; Olbrich, K. C.; McIntosh, T.; Needham, D.; Evans, E. Effect of chain length and unsaturation on elasticity of lipid bilayers. Biophysical Journal. 79. (2000) 328-39.

[23] Zhang, Y. W.; Lervik, A.; Seddon, J.; Bresme, F. A coarse-grained molecular dynamics investigation of the phase behavior of DPPC/cholesterol mixtures. Chemistry and Physics of Lipids. 185(2015) 88–98.

[24] Nagle, J. F. Theory of the Main Lipid Bilayer Phase Transition. Ann. Rev. Phys. Chem. 1980. 31:157-95.

[25] Marrink, S. J.; de Vries, A. H.; Mark, A. E. Coarse Grained Model for Semiquantitative Lipid Simulations. J. Phys. Chem. B 2004, 108, 750-760.

[26] Marrink, S. J.; Risselada, H. J.; Yefimov, S.; Tieleman, D. P.; de Vries, A. H. The MARTINI Force Field: Coarse Grained Model for Biomolecular Simulations. J. Phys. Chem. B 2007, 111, 7812-7824.

[27] Arnarez, C.; Uusitalo, J.; Masman, M.; Ingólfsson, H. I.; de Jong, D.; Melo, M.; Periole, X.; de Vries, A.; Marrink, S. DRY MARTINI, a Coarse-Grained Force Field for Lipid Membrane Simulations with Implicit Solvent. J. Chem. Theory Comput. 2015, 11, 260−275.

[28]Lee, H.; de Vries, A. H.; Marrink, S.-J. J.; Pastor, R. W. A Coarse-Grained Model for Polyethylene Oxide and Polyethylene Glycol: Conformation and Hydrodynamics. J. Phys. Chem. B 2009, 113, 13186−13194.

[29] Yang, S. C.; Faller, R. Pressure and Surface Tension Control Self-Assembled Structures in Mixtures of Pegylated and Non-Pegylated Lipids. Langmuir 2012, 28, 2275.2280.

[30] Wang S. H.; Larson, R. G. A Coarse-Grained Implicit Solvent Model for Poly(ethylene oxide),CnEm Surfactants, and Hydrophobically End-Capped Poly(ethylene oxide) and Its Application to Micelle Self-Assembly and Phase Behavior. Macromolecules 2015, 48, 7709−7718.

[31] Allen, M. P.; Tildesley, D. J. Computer Simulation of Liquids. Oxford : Clarendon Press, 1987.

[32]. Frenkel, D.; Smit, B. Understanding Molecular Simulation: From Algorithms to Applications. 2nd. San Diego : Academic Press, 2002.

[33]Plimpton, S. Fast Parallel Algorithms for Short-Range Molecular Dynamics. J. Comput. Phys. 1995, 117 (1), 1–19.

[34] Ahmed, A. Sadus, R. J. Phase diagram of the Weeks-Chandler-Andersen potential from very low to high temperatures and pressures. PHYSICAL REVIEW E 80, 061101 (2009).

[35] Guo, Y. C.; Baulin, V. A. General model of phospholipid bilayers in fluid phase within the single chain mean field theory. J Chem Phys. 2014 May 7;140(17):174903.

[36] Devanand, K.; Selser, J. C. Asymptotic Behavior and Long-Range Interaction in Aqeuous Solutions of Poly(ethylene oxide). Macromolecules 1991, 24, 5943-5947.

[37] Vermeer, L. S.; Bert, L. G.; Re´at, V.; Milon, A.; Czaplicki, J. Acyl chain order parameter profiles in phospholipid bilayers: computation from molecular dynamics simulations and comparison with $^{2}$H NMR experiments. Eur Biophys J (2007) 36:919–931.

[38] TORRIE, G. M.; VALLEAU, J. P. Nonphysical Sampling Distributions in Monte Carlo Free-Energy Estimation: Umbrella Sampling. JOURNAL OF COMPUTATIONAL PHYSICS 23, 187-199 (1977).

[39] Wang S. H.; Larson, R. G. Coarse-Grained Molecular Dynamics Simulation of Self-Assembly and Surface Adsorption of Ionic Surfactants Using an Implicit Water Model. Langmuir 2015, 31, 1262-1271.